Adaptive Order Tracking Technique Using Recursive Least-Square Algorithm

Mingsian R. Bai
e-mail: msbai@cc.nctu.edu.tw

Jihjau Jeng

Chingyu Chen

Department of Mechanical Engineering,
National Chiao-Tung University,
1001 Ta-Hsueh Road, Hsin-Chu,
Taiwan 300, Republic of China

Order tracking technique is one of the important tools for diagnosis of rotating machinery. Conventional methods of order tracking are primarily based on Fourier analysis with reference to shaft speed. Resampling is generally required in the fast Fourier transform (FFT)-based methods to compromise between time and frequency resolution for varying shaft speeds. Conventional methods suffer from a number of shortcomings. In particular, smearing problems arise when closely spaced orders or crossing orders are present. Conventional methods also are ineffective for the applications involving multiple independent shaft speeds. This paper presents an adaptive order tracking technique based on the Recursive Least-Squares (RLS) algorithm to overcome the problems encountered in conventional methods. In the proposed method, the problem is treated as the tracking of frequency-varying bandpass signals. Order amplitudes can be calculated with high resolution by using the proposed method in real-time fashion. The RLS order tracking technique is applicable whether it is a single-axle or multi-axle system.
[DOI: 10.1115/1.1501301]

1 Introduction

Rotating machinery represents an important class of mechanical systems. For example, compressors, pumps, fans, motors, generators and engines in factories and vehicles all fall into this category. Common causes of vibration in rotating machinery are imbalance, misalignment, looseness, bearing fault, gear fault, resonance, and so forth [1]. Apart from resonance, these common causes can be related to the rotating speed of the shaft. Rotor faults may result in excessive vibration which will in turn produce adverse effects on noise, reliability and performance of machines.

The condition of rotating machine can be monitored by measuring the noise or vibration signals at certain locations, e.g., bearing mounts. These signals generally consist of harmonics, most of which can be related to shaft speed. Among the methods devoted to diagnosis of rotor faults, an order tracking technique that exploits noise or vibration signals supplemented with information of shaft speed serves as an important tool for diagnosis of rotating machinery. More accurate interpretation of noise and vibration signature can be obtained by converting the frequency spectra into the so-called order spectra, with the "order" defined as the frequency normalized by the shaft speed. An order spectrum gives the amplitude of signal as a function of harmonic order and shaft speed (in rpm). The relationship between order analysis and frequency analysis is summarized in Table 1. Conventional methods of order tracking are primarily based on Fourier analysis, where narrow-band spectra of the frequency-varying signals are calculated by using time-windowing approach [2]. Resampling is generally required in the Fast Fourier transform (FFT)-based methods to compromise between time and frequency resolution for various shaft speeds. However, conventional FFT methods suffer from a number of shortcomings. In particular, the smearing problem may arise in two situations. First, orders can be closely spaced, particularly at low shaft speed. Second, undesirable beating may occur due to the crossing of speed-dependent orders and constant frequency components resulting from resonance or asynchronous rotation. In addition, conventional methods are ineffective for applications involving multiple independent shaft speeds. For example, the speed of the crankshaft of an engine and the speed of the

cooling fan are independent. If one calculates the orders based on either speed, the signal related to the other speed would appear as uncorrelated noise and affect the tracking accuracy of the results.

In order to avoid the aforementioned problems encountered in the conventional methods, model-based methods have been proposed. A representative example is the Vold-Kalman method [3,4]. In this method, the order tracking problem is formulated in terms of state space models. Order amplitudes are calculated off-line by using a least-squares approach. The method is based on a fixed sampling rate and generally implemented as a post-processing scheme.

In this paper, a model-based method is proposed for tracking the orders of noise and vibration signal of rotating machinery. This technique exploits adaptive filtering based on the Recursive Least-Squares (RLS) algorithm, where the problem is treated as the tracking of frequency-varying bandpass signals. Similar to conventional methods, the proposed method also requires information of shaft speed measured by a tachometer or an encoder. The algorithm is essentially sample-based and thus order amplitudes can be calculated in real-time fashion. In addition, the proposed technique is applicable either as a single-axle or multi-axle system. Unlike conventional methods, the proposed technique has no slew rate limitation provided the shaft speed is accurately estimated. Extensive simulation has been undertaken to compare the proposed technique to the FFT-based methods without and with tracking, and a Least-Squares (LS) block processing method. The results indicate that the proposed method is well suited for the tracking of closely spaced orders or crossing orders, without significant smearing.

2 Conventional Order Tracking Method

Conventional order analysis is generally based on the following Discrete Fourier transform (DFT) [5]:

$$X(k) = \sum_{n=0}^{N-1} x(n) W_n^{kn}, \quad 0 \leq k \leq N-1, \tag{1}$$

$$x(n) = \frac{1}{N} \sum_{k=0}^{N-1} X(k) W_N^{-kn}, \quad 0 \leq n \leq N-1, \tag{2}$$

Table 1 Relation between conventional frequency analysis and order tracking analysis

	Conventional Frequency Analysis	Order Tracking Analysis
Signal	Time (sec)	Revolutions (rev)
Spectrum	Frequency (Hz) (per sec)	Harmonics (order) (per rev)

where $x(n)$, $0 \leq n \leq N-1$ are discrete-time samples, $X(k)$, $0 \leq k \leq N-1$ are the DFT of $x(n)$, and $W_N = e^{-j(2\pi/N)}$. In practice, the computation of DFT is efficiently carried out by the FFT algorithm [5]. An appropriate sampling rate must be selected to process a nonstationary signal. To avoid leakage, time windows such as the Hanning window can be applied to the original sequence. Because the window is moving, the method is sometimes called the short-time Fourier transform (STFT) [6]:

$$X_{STFT}(e^{j\omega},m) = \sum_{n=-\infty}^{\infty} x(n)\nu(n-m)e^{-j\omega n}, \qquad (3)$$

where ω is the digital frequency and the finite-length window $\nu(n)$ is shifted with the discrete-time variable m.

In this paper, two FFT-based order analysis methods are presented. The first method is referred to as *FFT without tracking*. This method simply employs a fixed sampling rate method without the reference to the shaft speed. The second method is referred to as *FFT with tracking*. This method employs a resampling scheme synchronous with the shaft speed. Within a revolution, the noise or vibration signal is resampled with N points. The time-domain data are hence converted to revolution-domain data shown in Fig. 1. FFT is then applied for obtaining the order spectrum with respect to shaft speed. The requirement of time and frequency resolution of this approach is determined by shaft speed. At low speeds, low sampling rate (above twice the rotation frequency) is sufficient to capture the signal within several cycles. At high speed, on the other hand, a high sampling rate is generally used to capture the fast varying signal. For a fixed number of samples in FFT calculations, small time resolution gives large frequency resolution. The trade-off between the time and frequency resolutions is referred to as the Heisenberg's uncertainty principle [5].
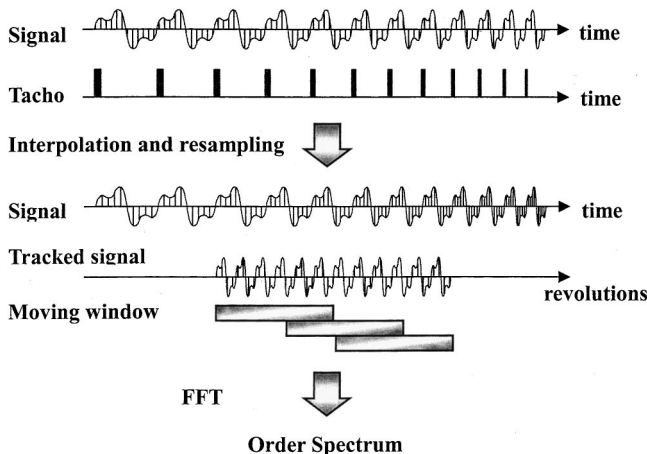

Fig. 1 Schematic of the method FFT with tracking

3 High Resolution Algorithms of Order Tracking Technique

3.1 Least-square Block Processing. In this section, an order tracking technique based on LS block processing is introduced. In general, the vibration signal generated by rotating machinery is essentially a frequency-modulated bandpass signal [7] and can be represented as the superposition of sinusoids. For instance, the noise or vibration signal $x(t)$ containing k orders generated by one rotating shaft can be written as

$$x(t) = A_1 \cos[\theta(t)+\phi_1] + A_2 \cos[2\theta(t)+\phi_2] + \cdots$$
$$+ A_k \cos[k\theta(t)+\phi_k], \qquad (4)$$

where A_k and ϕ_k represent the amplitude and phase, respectively, of the kth order, and the variable $\theta(t)$ denotes the angular displacement of the rotating shaft, as calculated by numerically integrating the instantaneous angular frequency measured by the tachometer.

$$\theta(t) = \int_0^t \omega(\tau)d\tau = \int_0^\tau 2\pi f(\tau)d\tau, \qquad (5)$$

where $\omega(t)$ represents the instantaneous angular frequency (rad/sec) of the rotating shaft. By trigonometric identity, Eq. (4) can be expanded as

$$x(t) = A_{1I}\cos[\theta(t)] - A_{1Q}\sin[\theta(t)] + A_{2I}\cos[2\theta(t)]$$
$$- A_{2Q}\sin[2\theta(t)] + \cdots + A_{kI}\cos[k\theta(t)] - A_{kQ}\sin[k\theta(t)], \qquad (6)$$

where A_{kI} and A_{kQ} denote the in-phase and quadrature components, respectively, of the kth order. Note that

$$A_{kI} = A_k \cos \phi_k, \qquad A_{kQ} = A_k \sin \phi_k. \qquad (7)$$

The amplitude and the phase of the kth order can be written as

$$|A_k| = \sqrt{A_{kI}^2 + A_{kQ}^2}, \qquad (8)$$

and

$$\phi_k = \tan^{-1}\left(\frac{A_{kQ}}{A_{kI}}\right). \qquad (9)$$

Equation (6) can be expressed as

$$x(t) = [\cos[\theta(t)] - \sin[\theta(t)]\cos[2\theta(t)]$$

$$-\sin[2\theta(t)]\cdots\cos[k\theta(t)] - \sin[k\theta(t)]]\begin{bmatrix} A_{1I} \\ A_{1Q} \\ A_{2I} \\ A_{2Q} \\ \vdots \\ A_{kI} \\ A_{kQ} \end{bmatrix} \qquad (10)$$

Discretization of Eq. (10) leads to

$$x(n) = [\cos[\theta(n)] - \sin[\theta(n)]\cos[2\theta(n)]$$

$$-\sin[2\theta(n)]\cdots\cos[k\theta(n)] - \sin[k\theta(n)]]\begin{bmatrix} A_{1I} \\ A_{1Q} \\ A_{2I} \\ A_{2Q} \\ \vdots \\ A_{kI} \\ A_{kQ} \end{bmatrix}$$
$$\qquad (11)$$

where n is the discrete-time index.

To solve Eq. (11), we collect $2k$ samples of $x(n)$ to form

$$
\begin{bmatrix} x(n) \\ x(n+1) \\ \vdots \\ x(n+2k-2) \\ x(n+2k-1) \end{bmatrix} = \begin{bmatrix} \cos[\theta(n)] & -\sin[\theta(n)] & \cdots & \cos[k\theta(n)] & -\sin[k\theta(n)] \\ \cos[\theta(n+1)] & -\sin[\theta(n+1)] & \cdots & \cos[k\theta(n+1)] & -\sin[k\theta(n+1)] \\ \vdots & \vdots & \cdots & \vdots & \vdots \\ \cos[\theta(n+2k-2)] & -\sin[\theta(n+2k-2)] & \cdots & \cos[k\theta(n+2k-2)] & -\sin[k\theta(n+2k-2)] \\ \cos[\theta(n+2k-1)] & -\sin[\theta(n+2k-1)] & \cdots & \cos[k\theta(n+2k-1)] & -\sin[k\theta(n+2k-1)] \end{bmatrix} \begin{bmatrix} A_{1I} \\ A_{1Q} \\ \vdots \\ A_{kI} \\ A_{kQ} \end{bmatrix}
$$

$$(12)$$

Here we assume that the $2k$ amplitude parameters A_I and A_Q remain constant within the interval $[n, n+2k-1]$. Equation (12) can be written in the following matrix form

$$\mathbf{x} = \Theta \mathbf{a}, \qquad (13)$$

where $\mathbf{x}$ is $2k \times 1$ vector consisting of $2k$ signal samples, and Θ is $2k \times 2k$ matrix consisting of angular displacements of the rotating shaft. The $2k \times 1$ vector $\mathbf{a}$ in Eq. (13) involves parameters for the identification of the amplitudes of k orders. From Eq. (13), the amplitudes can be solved by inverting the matrix Θ

$$\mathbf{a} = \Theta^{-1} \mathbf{x}. \qquad (14)$$

By using Eq. (8), the amplitudes of the k orders in the interval $[n, n+2k-1]$ can be calculated. In practice, pseudoinversion of the matrix Θ may have to be used for high sampling rate cases in which the matrix Θ is nearly singular.

For multiple-axle applications, the aforementioned LS block processing algorithm can be easily extended. For instance, the noise or vibration signal $x(t)$ containing k orders generated by a two-shaft system is written as

$$
\begin{aligned}
x(t) = & A_1 \cos[\theta(t) + \phi_1] + A_2 \cos[2\theta(t) + \phi_2] \\
& + \cdots + A_k \cos[k\theta(t) - \phi_k] + A_1' \cos[\theta'(t) + \phi_1'] \\
& + A_2' \cos[2\theta'(t) + \phi_2'] + \cdots + A_l' \cos[l\theta'(t) + \phi_l'],
\end{aligned}
$$

$$(15)$$

where A_k and A_k' represent the amplitudes of the kth order of each axle, ϕ_k and ϕ_k' represent the phases of the kth order of each axle. The variable $\theta(t)$ and $\theta'(t)$ denote the angular displacements of each axle. The angular displacements are computed by the following integrals

$$\theta(t) = \int_0^t \omega(\tau) d\tau = \int_0^t 2\pi f(\tau) d\tau \qquad (16)$$

and

$$\theta'(t) = \int_0^t \omega'(\tau) d\tau = \int_0^t 2\pi f'(\tau) d\tau, \qquad (17)$$

where $\omega(t)$ and $\omega'(t)$ represent the instantaneous angular frequencies (rad/sec) of these two "independent" shafts, respectively. Similarly, the amplitude of the k orders of each shaft can be solved as

$$\mathbf{a} = \Theta^{-1} \mathbf{x}, \qquad (18)$$

where $\mathbf{x}^T = [x(n) x(n+1) \cdots x(n+4k-2) x(n+4k-1)]$

$$(19)$$

is a $4k \times 1$ matrix containing $4k$ samples. The matrix

$$\Theta = [\Theta_1 \Theta_2] \qquad (20)$$

is a $4k \times 4k$ matrix containing angular displacements of both shafts, where

$$
\Theta_1 = \begin{bmatrix} \cos[\theta(n)] & -\sin[\theta(n)] & \cdots & \cos[\theta(n)] & -\sin[\theta(n)] \\ \cos[\theta(n+1)] & -\sin[\theta(n+1)] & \cdots & \cos[\theta(n+1)] & -\sin[\theta(n+1)] \\ \vdots & \vdots & \cdots & \vdots & \vdots \\ \cos[k\theta(n+4k-2)] & -\sin[k\theta(n+4k-2)] & \cdots & \cos[k\theta(n+4k-2)] & -\sin[k\theta(n+4k-2)] \\ \cos[k\theta(n+4k-1)] & -\sin[k\theta(n+4k-1)] & \cdots & \cos[k\theta(n+4k-1)] & -\sin[k\theta(n+4k-1)] \end{bmatrix}
$$

and

$$
\Theta_2 = \begin{bmatrix} \cos[\theta'(n)] & -\sin[\theta'(n)] & \cdots & \cos[\theta'(n)] & -\sin[\theta'(n)] \\ \cos[\theta'(n+1)] & -\sin[\theta'(n+1)] & \cdots & \cos[\theta'(n+1)] & -\sin[\theta'(n+1)] \\ \vdots & \vdots & \cdots & \vdots & \vdots \\ \cos[k\theta'(n+4k-2)] & -\sin[k\theta'(n+4k-2)] & \cdots & \cos[k\theta'(n+4k-2)] & -\sin[k\theta'(n+4k-2)] \\ \cos[k\theta'(n+4k-1)] & -\sin[k\theta'(n+4k-1)] & \cdots & \cos[k\theta'(n+4k-1)] & -\sin[k\theta'(n+4k-1)] \end{bmatrix}.
$$

The $4k \times 1$ vector

$$\mathbf{a}^T = [A_{1I} \; A_{1Q} \; \cdots \; A_{kI} \; A_{kQ} \; A_{1I}' \; A_{1Q}' \; \cdots \; A_{kI}' A_{kQ}'] \qquad (21)$$

consists of amplitudes of the k orders to be identified.

3.2 RLS Order Tacking Algorithm. Although the aforementioned LS block processing algorithm is straightforward, it suffers from two problems. Not only must it be implemented off-line because of its batch-processing nature but also it is suscep-

tible to noise. Thus, it is only regarded as a benchmark method in this paper. In this section, an adaptive approach based on RLS filtering, which essentially avoids the problem of the LS block processing, is presented. In light of the special structure of the signal described in Eq. (6), the order tracking problem can be recast into a parameter identification problem. The estimation error of the model is written as

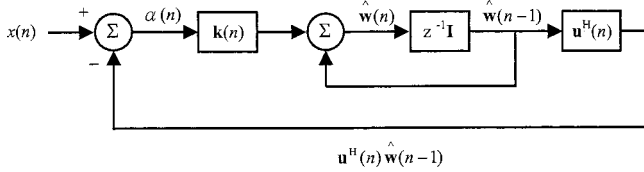$$e(n) = x(n) - \mathbf{w}^T(n) \mathbf{u}(n), \qquad (22)$$

Fig. 2 Block diagram of the RLS algorithm

where n is the discrete-time index,

$$\mathbf{u}^T(n) = [\cos[\theta(n)] - \sin[\theta(n)]\cos[2\theta(n)]$$
$$- \sin[2\theta(n)] \cdots \cos[k\theta(n)] - \sin[k\theta(n)]] \quad (23)$$

is the regressor,

$$\mathbf{w}^T(n) = [A_{1I}(n)A_{1Q}(n)A_{2I}(n)A_{2Q}(n) \cdots A_{nI}(n)A_{kQ}(n)] \quad (24)$$

is the parameter vector, and $x(n)$ is the measurement. The vector $\mathbf{u}(n)$ consists of angular displacements of the shaft, while the vector $\mathbf{w}(n)$ consists of the in-phase and quadrature components of all orders to be identified.

The parameter identification problem in Eq. (22) can be solved by the method of least squares. The problem amounts to finding optimal parameters $\hat{\mathbf{w}}(n)$ such that the following performance index $\zeta(n)$ is minimized

$$\zeta(n) = \sum_{i=1}^{n} \lambda^{n-i} |e(i)|^2, \quad (25)$$

where the forgetting factor λ weighs exponentially the estimation error from the present to the past. The optimal solution to problem can be recursively solved by using the following RLS algorithm [8].

$$\mathbf{k}(n) = \frac{\lambda^{-1}\mathbf{P}(n-1)\mathbf{u}(n)}{1 + \lambda^{-1}\mathbf{u}^H(n)\mathbf{P}(n-1)\mathbf{u}(n)}, \quad (26)$$

$$\alpha(n) = x(n) - \hat{\mathbf{w}}^H(n-1)\mathbf{u}(n), \quad (27)$$

$$\hat{\mathbf{w}}(n) = \hat{\mathbf{w}}(n-1) + \mathbf{k}(n)\alpha^*(n), \quad (28)$$

$$\mathbf{P}(n) = \lambda^{-1}\mathbf{P}(n-1) - \lambda^{-1}\mathbf{k}(n)\mathbf{u}^H(n)\mathbf{P}(n-1). \quad (29)$$
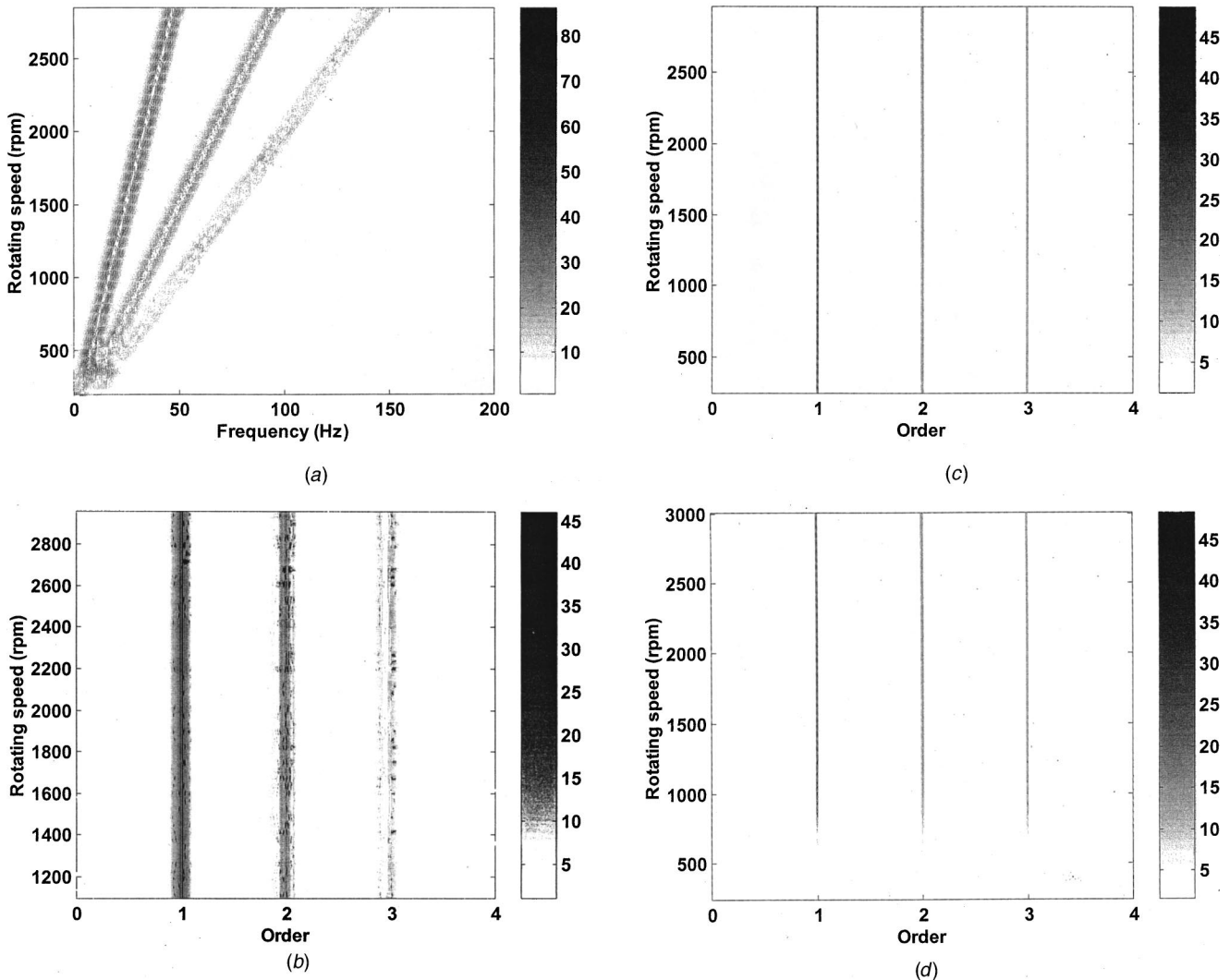

(a)

(c)

(b)

(d)

Fig. 3 Contour plots obtained using the order tracking methods for the slew rate 20 Hz/sec: (a) FFT without tracking ; (b) FFT with tracking; (c) LS block processing; (d) RLS algorithm.

Table 2 Summary of the parameters in simulation cases

	Slew rate (Hz/sec)		N_{order}	$\hat{N}_{order}$	λ
	axle 1	axle 2			
Case 1	20	--	3	3	0.995
	100	--	3	3	0.99085
Case 2	60	--	3	3	0.995
Case 3	60	--	3	3	0.995
Case 4	60	--	3	5	0.995
	60	--	3	1	0.994
Case 5	60	33	6	6	0.994

In this procedure, the matrix $\mathbf{P}(n)$ is the inverse of auto-correlation matrix of input vector $\mathbf{u}$, $\alpha(n)$ is the *a priori* estimation error, and $\mathbf{k}(n)$ is the gain vector. To initialize the RLS algorithm, the initial conditions are generally taken to be: $\hat{\mathbf{w}}(0) = 0_{M \times 1}$ (M is the number of parameters), $\mathbf{P}(0) = \delta^{-1}\mathbf{I}$ ($\mathbf{I}$ is a $M \times M$ identity matrix), and δ is a small positive constant. Figure 2 shows the block diagram of RLS algorithm.

There are two possible extensions to the RLS order tracking technique. First, the method can be easily extended to multi-axle applications involving more than one independent fundamental frequency. This situation often arises in many practical applications, e.g., belt slippage or cooling fan. Second, constant frequency components can be incorporated to the formulation of parameter identification. This constant frequency component represents the effects due to resonance or an asynchronous signal that is constantly present, e.g., electrical noise present in a signal from a machine whose speed is not at grid frequency. For example of a two-axle system with one constant frequency component at f_R, Eq. (4) should be modified into
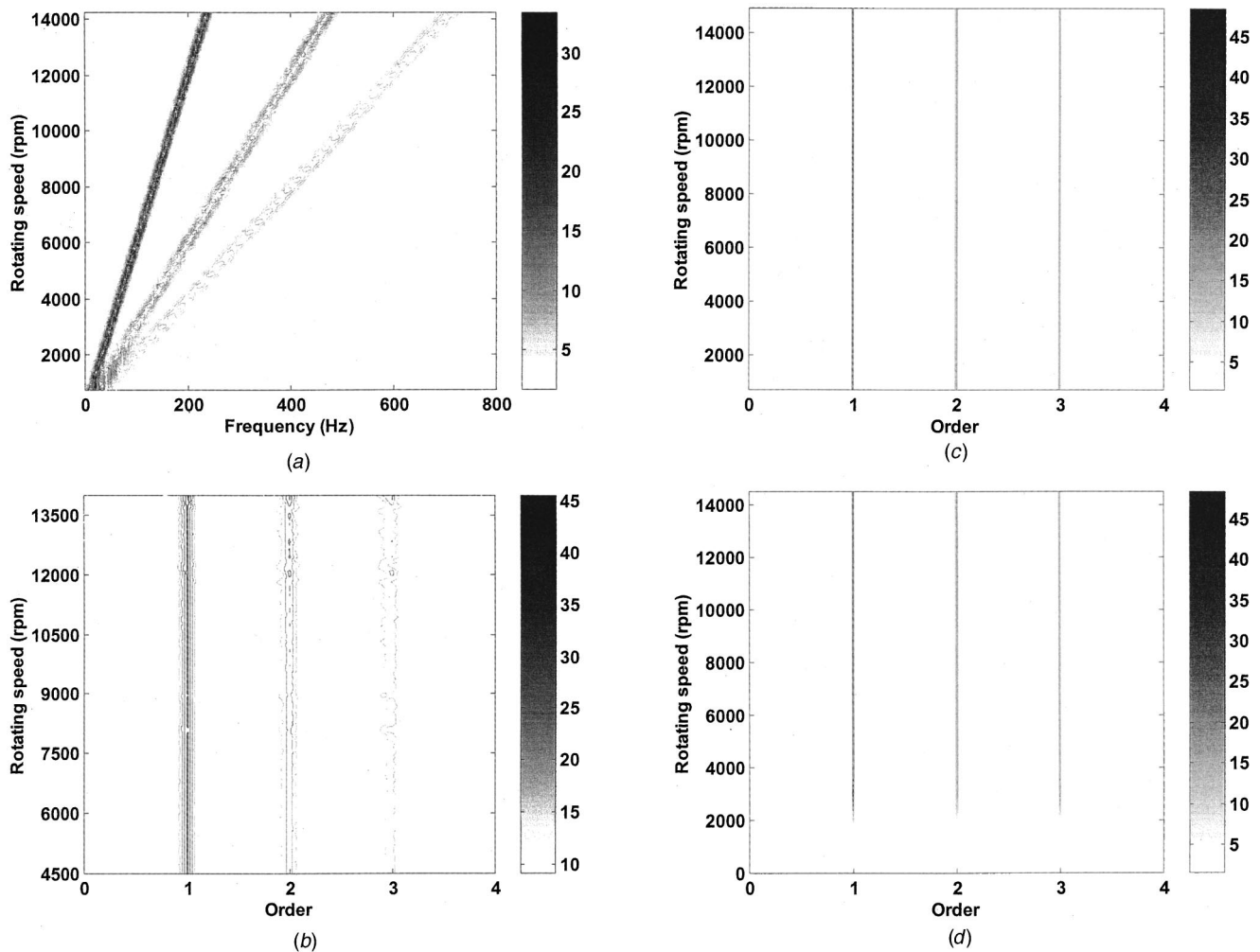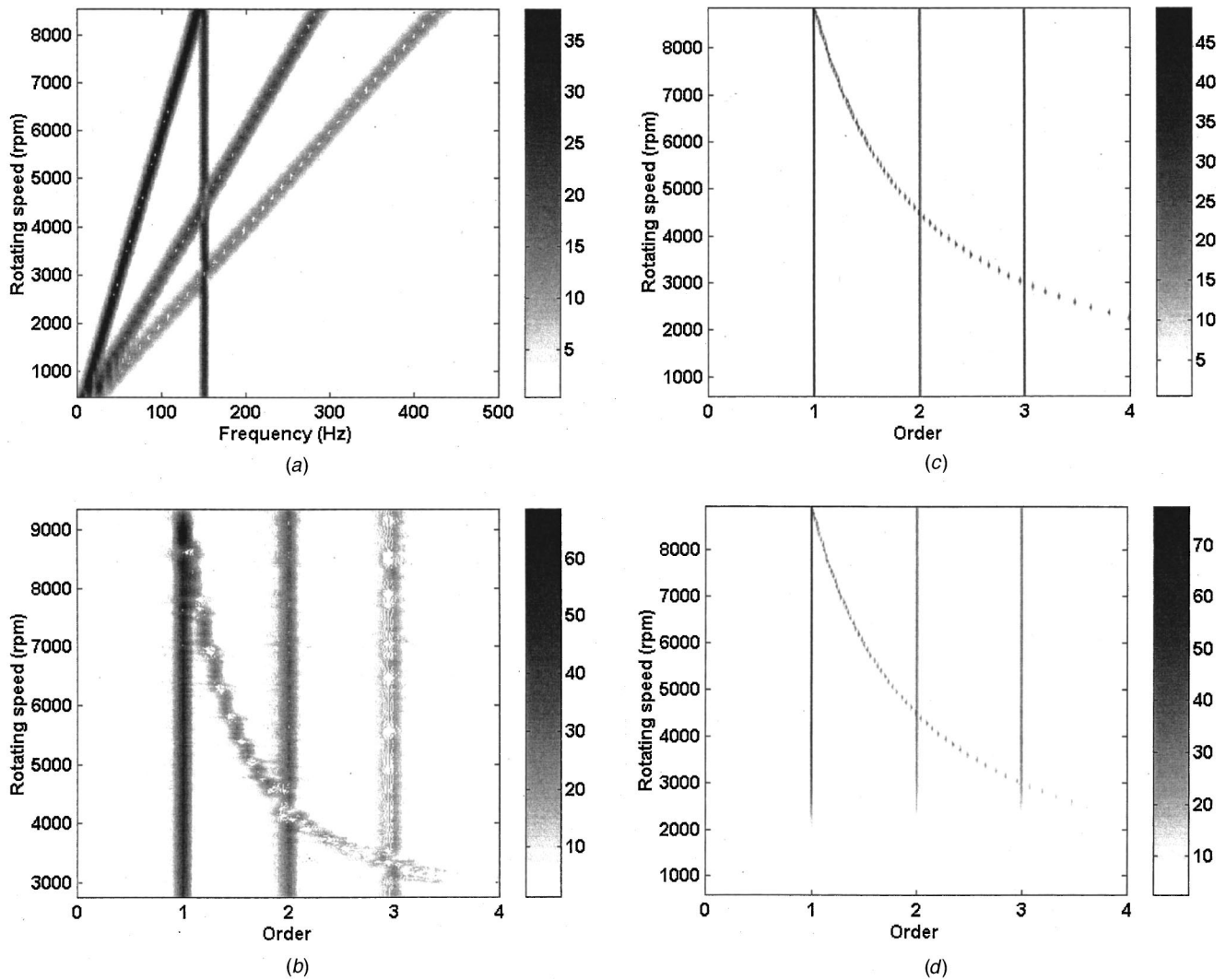

Fig. 4 Contour plots obtained using the order tracking methods for the slew rate 100 Hz/sec: (*a*) FFT without tracking; (*b*) FFT with tracking; (*c*) LS block processing; (*d*) RLS algorithm.

Fig. 5 Contour plots obtained using the order tracking methods for testing the effect of constant frequency component: (*a*) FFT without tracking; (*b*) FFT with tracking; (*c*) LS block processing; (*d*) RLS algorithm.

$$x(t) = A_1 \cos[\theta(t) + \phi_1] + A_2 \cos[2\theta(t) + \phi_2]$$

$$+ \cdots + A_k \cos[k\theta(t) + \phi_k] + A'_1 \cos[\theta'(t) + \phi'_1]$$

$$+ A'_2 \cos[2\theta'(t) + \phi'_2] + \cdots + A'_m \cos[m\theta'(t) + \phi'_m]$$

$$+ A_R \cos(2\pi f_R t + \phi_R), \tag{30}$$

where $\theta(t)$ and $\theta'(t)$ denote angular displacements of axle 1 and axle 2, respectively, ϕ's are the corresponding phases, A_i and A'_i represent the amplitudes of axle 1 and axle 2, respectively, k and m are number of orders, and the A_R and f_R denote the amplitude and frequency of a constant frequency component, respectively. It is noted that, in applying this method, the shaft speed of each axle must be available. In addition, prior information of the number of order and the constant frequency component is also required. Technically, this can be obtained by a preliminary scan using the conventional order tracking methods. If this can be done, the proposed technique should provide results with improved accuracy. On the other hand, performance of the presented method will be affected if the number of order and the constant frequency are inaccurately estimated. The effects of the error in estimating these parameters will be explored in the following section.

4 Numerical Simulations and Discussions

Numerical simulations are carried out for the verification of the RLS order tracking algorithm.

4.1 Case 1: Run-up Test. This case simulates a run-up test of a single-axle system with constant slew rate f_{slew}. The measurement data involve three orders. The slew rates are assumed to be 20 Hz/sec and 100 Hz/sec, respectively. The measurement data is expressed as

$$x(t) = 20 \sin[\theta(t) + \phi_1] + 15 \sin[2\theta(t) + \phi_2] + 5 \sin[3\theta(t) + \phi_3], \tag{31}$$

where the angular displacement $\theta(t)$ is computed by the following integral

$$\theta(t) = \int_0^t 2\pi(f_{\text{slew}}\tau) d\tau = \pi f_{\text{slew}} t^2. \tag{32}$$

In the test, 5120 samples of $x(n)$ are generated, with sampling frequency 2048 Hz. Figure 3(*a*) shows the contour plot obtained using the FFT method without tracking for the slew rate 20 Hz/sec. The window length is chosen to be 512 samples with a 75% overlap. Smearing effect arises in the region of low shaft speed.
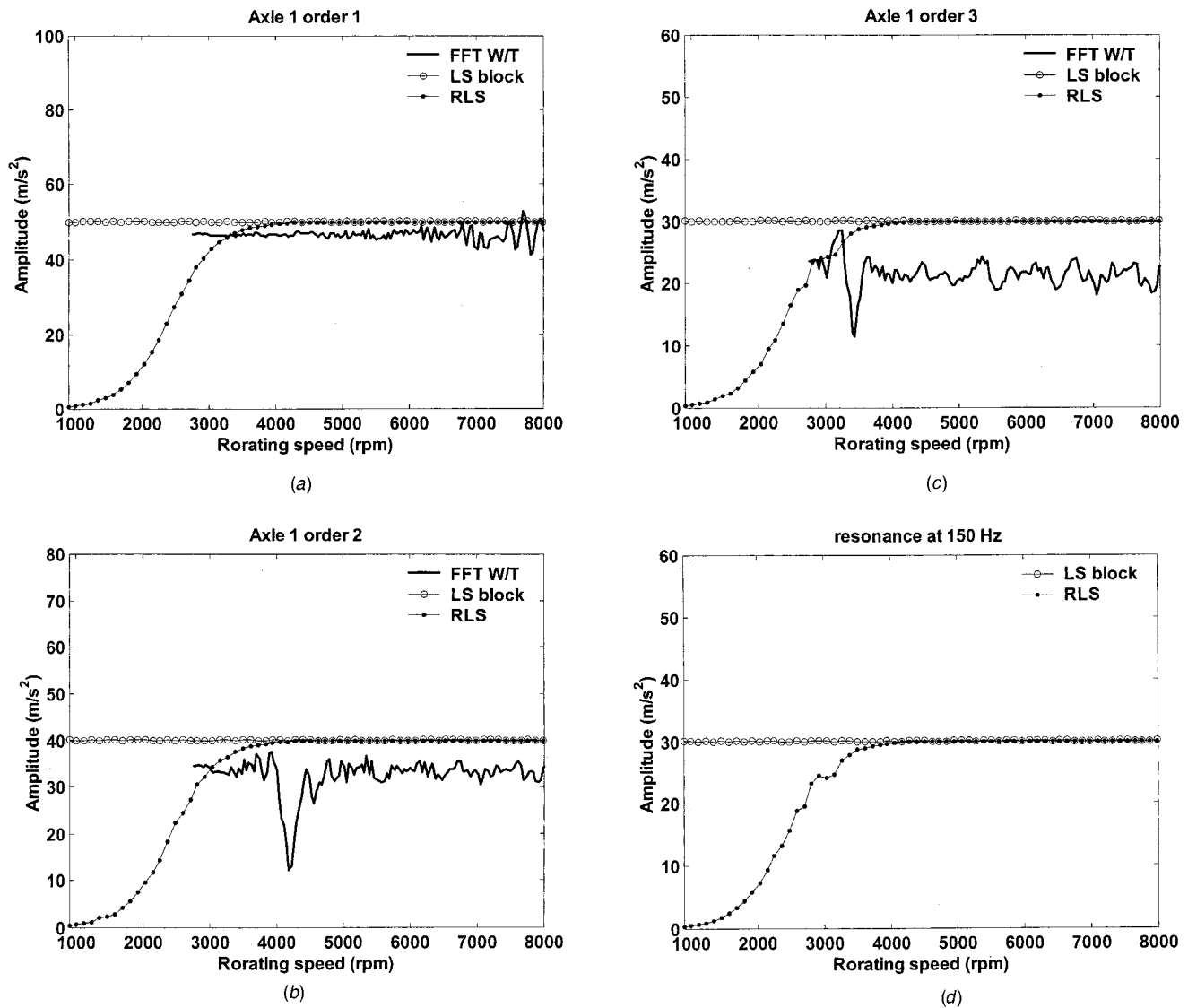
Fig. 6 Estimation of amplitudes using order tracking methods for testing the effect of constant frequency component: (a) Amplitude of order 1; (b) amplitude of order 2; (c) amplitude of order 3; (d) amplitude of constant frequency component.

Figure 3(b) shows the contour plots obtained using the FFT method with tracking for the slew rate 20 Hz/sec. Within each revolution, the measurement signal is resampled into 26 samples. The window length is chosen to be 10 revolutions, which amounts to 260 revolution-domain samples in a record. The overlapping percentage between windows is 90% in terms of revolutions. The parameters such as the order number $\hat{N}_{order}$ and the forgetting factor λ are summarized in Table 2. Figures 3(c)–(d) display the contour plots obtained by using the LS block processing and the RLS algorithm for the slew rate 20 Hz/sec, respectively. In Fig. 3(d), a clear result begins to emerge above 500 rpm because of the transient learning nature of the RLS algorithm. For a much higher slew rate 100 Hz/sec, the contour plots obtained using four methods are shown in Fig. 4. From the results, the model-based methods show their ability in resolving close orders.

4.2 Case 2: Constant Frequency Component. In this case, the ability of the proposed methods in resolving crossing orders between speed-related orders and a constant frequency component is examined. The measurement signal is generated by a single-axle system with a constant frequency component at 150 Hz:

$$x(t) = 50 \sin[\theta(t) + \phi_1] + 40 \sin[2\,\theta(t) + \phi_2] + 30 \sin[3\,\theta(t) + \phi_3]$$
$$+ 30 \sin(2\,\pi 150 t). \tag{33}$$

Figures 5(a) and (b) show the contour plots obtained using the method FFT without and with tracking, respectively. Smearing of crossing orders can be observed in both plots. Figures 5(c) and (d) show the contour plots obtained using LS block processing and RLS algorithm, respectively. It is seen that smearing problem has been eliminated by the model-based methods. In these contour plots, the constant frequency component appears as a hyperbola described by

$$cn = 60f, \tag{34}$$

where c denotes the shaft speed (in rpm), n is the order number, and f is the frequency (in Hz).

Figure 6 shows the amplitude estimation versus rpm obtained using four order tracking methods. The result of RLS algorithm converges to the assumed value beyond 3500 rpm.
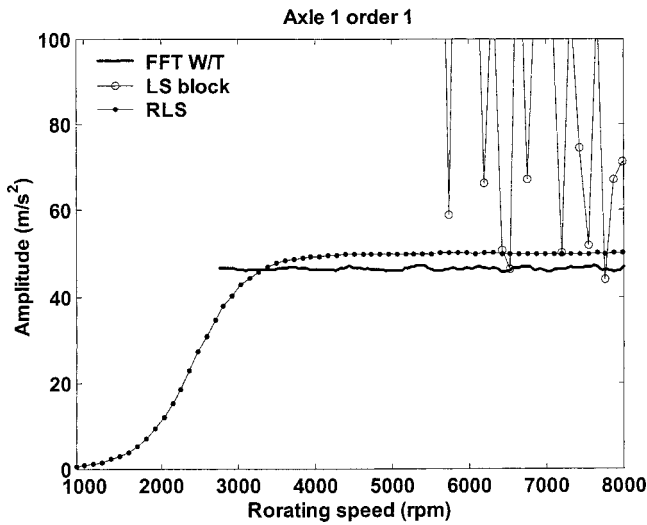
Fig. 7 Estimation of the amplitude of order 1 using the order tracking methods for testing the effect of noise

4.3 Case 3: Noise Effect. In practical applications, measurement noise always exists in data acquisition. In this subsection, the effect of measurement noise is examined. The test signal is given by

$$x(t) = 50 \sin[\theta(t) + \phi_1] + 40 \sin[2\theta(t) + \phi_2] + 30 \sin[3\theta(t) + \phi_3]$$

$$+ n(t). \tag{35}$$

The measurement noise $n(t)$ is a zero-mean white noise process with unity variance.

Figure 7 shows the amplitude estimation of order 1 by three order tracking methods. The result of the FFT method is somewhat biased due to leakage problem. The LS block processing method is extremely susceptible to measurement noise so that the result diverges completely. However, the result obtained using the RLS algorithm converges satisfactorily to the assumed values, regardless of the measurement noise.

4.4 Case 4: Order Estimation Error. The methods, LS block processing and RLS algorithm, are essentially model-based methods which requires the knowledge of order number, $\hat{N}_{order}$. This parameter is generally selected to be slightly larger than the actual order number, i.e.,

$$\hat{N}_{order} \geq N_{order}, \tag{36}$$

In practice, conventional FFT methods can be employed to get an idea of how many orders may be present in the measurement. In this subsection, the estimation error of order number is investigated. The order number $\hat{N}_{order}$ is assumed to be over-estimated and under-estimated, respectively, as shown in Table 2. The result of over-estimated case is presented in Fig. 8. RLS algorithm converges to the assumed values after 4000 rpm. The amplitudes of the ''over-estimated'' orders obtained using the model-based methods approach zero. Figure 9 shows the amplitude estimation of order 1 in the ''under-estimated'' case. The RLS method reaches the steady state, whereas the method LS block processing is found to be extremely susceptible to estimation error of order number and diverges completely. It is also remarked that the error in estimating the constant frequency component has a similar effect to the case of order number error. Both types of error result in incorrect model structure. The missed term in the model would behave like noise in adaptive estimation if it is omitted or in error.

4.5 Case 5: Multi-axle System. In this subsection, the ability of the proposed method in handling signal measured from a
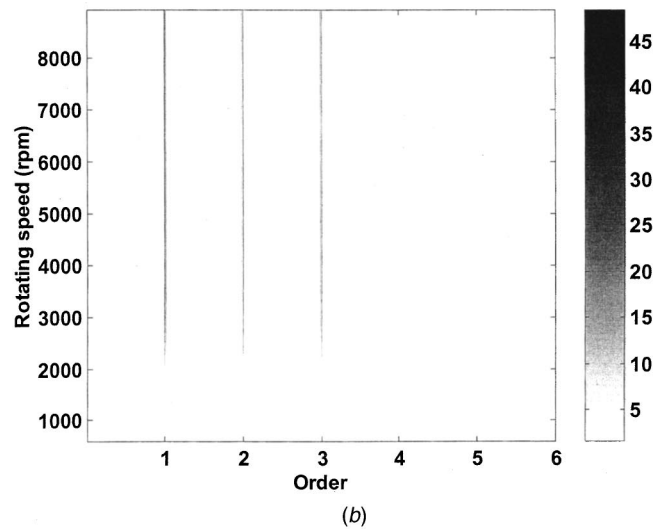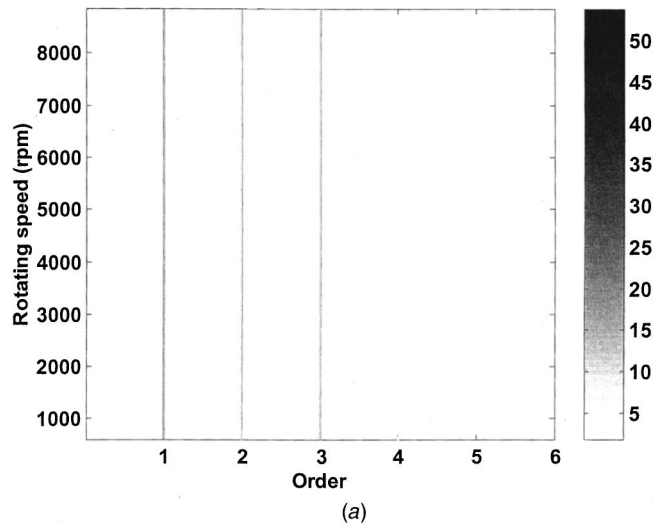

(a)

(b)

Fig. 8 Contour plots obtained using the model-based methods when the order number is over-estimated: (a) LS block processing; (b) RLS algorithm.
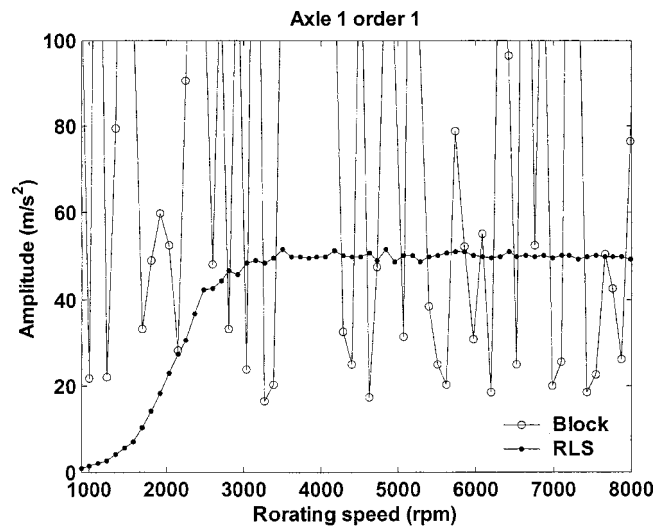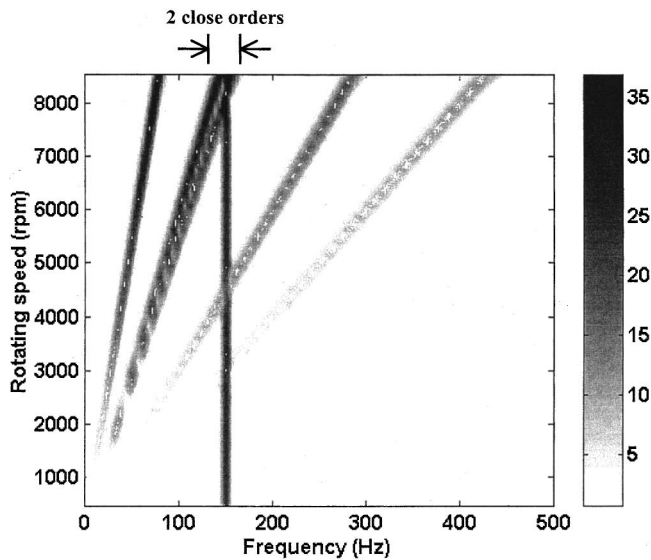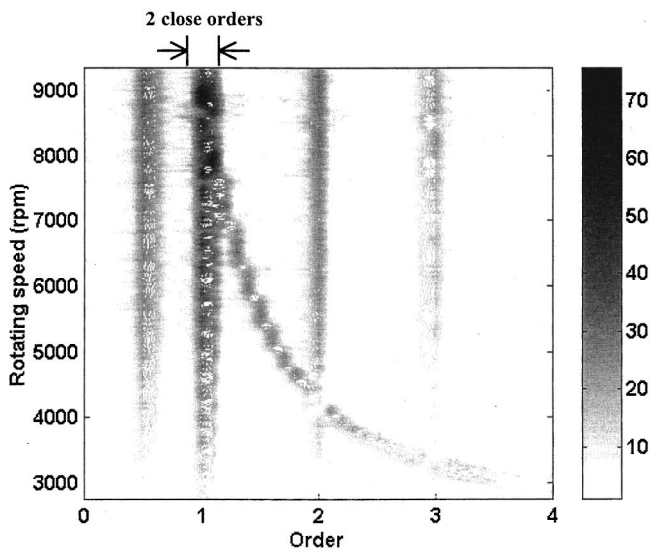

Fig. 9 Estimation of the amplitude of order 1 using the order tracking methods when the order number is under-estimated
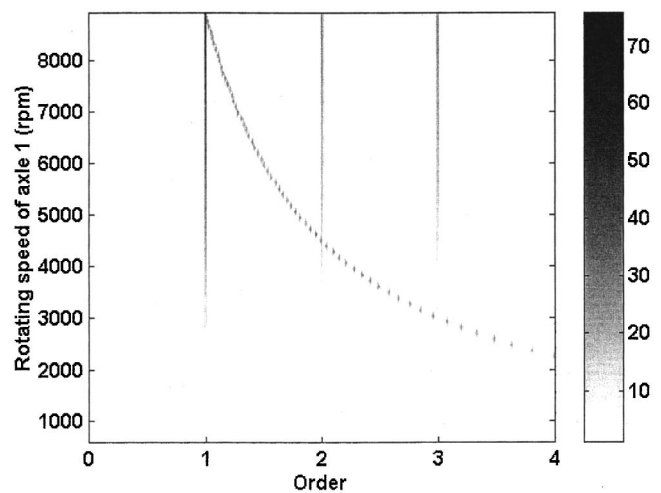
(a)

(b)

Fig. 10 Contour plots obtained using the FFT-based methods for tracking the orders of a two-axle system. The measurement signal involves time-varying amplitudes and one constant frequency component at 150 Hz: (a) FFT without tracking; (b) FFT with tracking.

multi-axle system is examined. A complex case involving time-varying amplitudes, two axles, a constant frequency component at 150 Hz is investigated

$$x(t) = 20t \sin[\theta(t) + \phi_1] + 16t \sin[2\theta(t) + \phi_2] + 12t \sin[3\theta(t)$$
$$+ \phi_3] + 20t \sin[\theta'(t) + \phi_1'] + 16t \sin[2\theta'(t) + \phi_2']$$
$$+ 30 \sin(2\pi150t). \tag{37}$$

Two shafts are rotating at independent frequencies according to $f(t) = 60t$ and $f'(t) = 33t$, respectively, which amounts to the fact the shaft speeds associated with the five terms of Eq. (37) are not constant but proportional to time. The variables $\theta(t)$ and $\theta'(t)$ are angular displacements. The variables ϕ_k and ϕ_k' represent the phase of the kth order of two shafts, respectively.

Figure 10(a) displays the contour plot obtained using the method FFT without tracking. Serious smearing prevents one

(a)
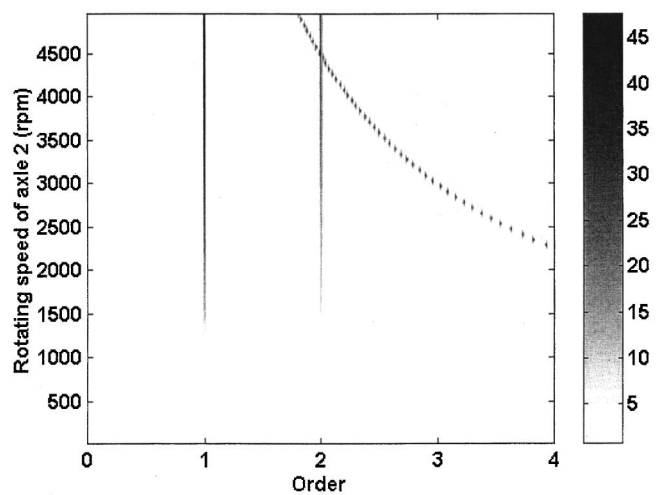
(b)

Fig. 11 Contour plots obtained using the RLS algorithm for tracking the orders of a two-axle system. The measurement signal involves time-varying amplitudes and one constant frequency component at 150 Hz: (a) Result of axle 1; (b) result of axle 2.
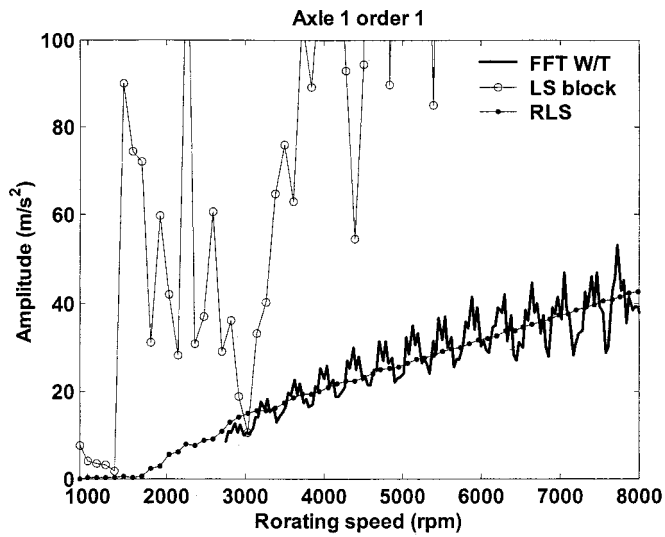
from resolving two very close orders, i.e., the 1st order of axle 1 and the 2nd order of axle 2. Figure 10(b) shows the result of the method FFT with tracking, using the tacho signal of the 1st axle as the reference. Three orders of axle 1 are clearly seen in the plot, while the orders of axle 2 are barely recognizable.

Figure 11 shows the contour plots obtained using the RLS algorithm. The hyperbola in the figure represents the constant frequency component. The orders of each axle are clearly recognized with the smearing problem completely eliminated.
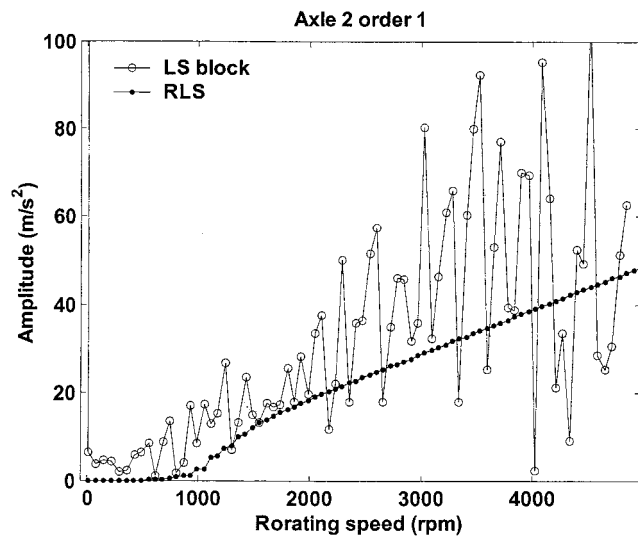
Figure 12 shows the amplitudes versus rpm of order 1 of axle 1 and order 1 of axle 2, respectively. Fluctuations are found in the results of FFT with tracking because only the tacho signal of axle 1 is used as the reference and the signal from axle 2 behaves like noise. The LS block processing is totally ineffective and diverges in this case. In contrast, the RLS algorithm remains effective in tracking the orders, even if close and crossing time-varying orders are present in the multi-axle system.

5 Conclusions

A model-based order tracking method based on the RLS algorithm has been presented to overcome the shortcomings of con-

Axle 1 order 1

(a)

Axle 2 order 1

(b)

Fig. 12 Estimation of the amplitudes using order tracking methods for tracking the orders of a two-axle system. The measurement signal involves time-varying amplitudes and one constant frequency component at 150 Hz: (a) Amplitude of order 1 of axle 1; (b) amplitude of order 1 of axle 2.

Table 3   Comparison of order tracking methods

Features	FFT without tracking	FFT with tracking	LS block processing	RLS algorithm
Need tacho. signal	No	Yes	Yes	Yes
Need resampling	No	Yes	No	No
Design parameters	No	No	$\hat{N}_{order}$	1. $\hat{N}_{order}$ 2. λ
Order estimation error	No	No	Yes	Yes
Memory requirement	Large	Large	Small	Small
Real time processing	No	No	No	Yes
Multi-axle	No	No	No	Yes
Noise effect	Yes	Yes	Yes	No
Time-varying amplitude	Bad	Bad	Bad	Good
Constant frequency component	No	No	Yes	Yes
Resolving close and crossing orders	No	No	No	Yes
Slew rate limitation	Yes	Yes	No	No

which a model structure must be established before implementation. The same situation occurs to other signal processing applications such as high-resolution spectral analysis and array signal processing. For these applications, estimates of the model structure should be obtained, based on the FFT scan or engineering judgment for certain classes of problems. For instance, if only imbalance and alignment are anticipated for a rotor system, then one would guess the order to be at least two. Nevertheless, this point is still worth exploring in a future study. As another limitation of the proposed method, like other adaptive filtering techniques, initial transients inevitably arise during the learning process of the RLS algorithm. The larger the forgetting factor, the longer are the transients. To cope with this problem, the authors' suggestion is to either dwell at a constant low speed until it settles and then increase the speed, or run another coast down test. The future work will also be focused on comparison with other adaptive filtering methods, e.g., Kalman filter and experimental verification.

References

[1] Ehrich, F. F., 1992, *Handbook of Rotordynamics*, McGraw-Hill, New York.
[2] Bandhopadhyay, D., K., and Griffiths, D., 1995, "Methods for Analyzing Order Spectra," SAE Paper Number 951273, pp. 313–318.
[3] Vold, H., and Leuridan, J., 1993, "High Resolution Order Tracking at Extreme Slew Rates, Using Kalman filters," SAE Paper Number 931288, pp. 219–226.
[4] Vold, H., Mains, M., and Blough, J., 1997, "Theoretical Foundations for High Performance Order Tracking with the Vold-Kalman Tracking Filter," SAE Paper Number 972007, pp. 1083–1088.
[5] Oppenheim, A. V., and Schafer, R. W., 1999, *Discrete-Time Signal Processing*, Prentice-Hall, Upper Saddle River, NJ.
[6] Vaidyanathan, P. P., 1993, *Multirate Systems and Filter Banks*, Prentice-Hall, Englewood Cliffs, NJ.
[7] Denbigh, P., 1998, *System Analysis and Signal Processing*, Addison Wesley, New York.
[8] Haykin, S., 1986, *Adaptive Filter Theory*, Prentice-Hall, Englewood Cliffs, NJ.

ventional methods. This method has been verified through simulations. The RLS algorithm proves to be capable of resolving close and crossing orders, without significant slew rate limitation. This technique is effective in tracking the orders due to independent axles. Table 3 summarizes the properties of the conventional method with the method presented in this paper.

As pointed out by the reviewer, the success of the method depends on a reasonable estimate of the number of orders present in the data. A pre-scanning by the FFT method may be required to obtain a preliminary idea of the number of orders. This may appear to be a serious limitation of the proposed method. However, this is also the common problem of all model-based methods for